

**Electric current noise in mesoscopic organic semiconductors induced by nuclear spin fluctuations**D. S. Smirnov  and A. V. Shumilin   
*Ioffe Institute, 194021 St. Petersburg, Russia* (Received 9 December 2020; revised 24 March 2021; accepted 29 March 2021; published 27 May 2021)

We demonstrate that the nuclear spin fluctuations lead to the electric current noise in mesoscopic samples of organic semiconductors, which show the pronounced magnetoresistance in weak magnetic fields. For the bipolaron and electron-hole mechanisms of organic magnetoresistance, the current noise spectrum consists of the high-frequency peak related to the nuclear spin precession in the Knight field of the charge carriers and the low-frequency peak related to the nuclear spin relaxation. The shape of the spectrum depends on the external magnetic and radio frequency fields, which allows one to prove the role of the nuclei in the magnetoresistance experimentally.

DOI: [10.1103/PhysRevB.103.195440](https://doi.org/10.1103/PhysRevB.103.195440)**I. INTRODUCTION**

Organic semiconductors represent a relatively new class of semiconductors and are currently attracting increasing interest. Although they are already successfully used in light-emitting diodes [1,2], organic solar cells [3–5], and other devices, their transport properties are not completely understood theoretically yet. Organic semiconductors are amorphous materials which consist of single molecules or short polymers. The transport in them typically operates via hopping of polarons between molecular orbitals [6,7]. It is quite similar to the hopping conductivity in inorganic semiconductors [8]. For this reason in this paper we use the notations of electrons, holes, and hopping sites.

A unique feature of organic semiconductors is the strong coupling between electric current and nuclear spins. It was shown experimentally back in 2003 that light emission from organic diodes can be significantly modified by application of magnetic fields as small as 100 mT [9]. Then in 2005 it was found that the resistivity of organic semiconductors can be affected by the magnetic fields in the same range [10]. This effect is called organic magnetoresistance (OMAR). It takes place in a number of different organic materials at liquid helium as well as at room temperatures.

Qualitatively, OMAR is related to the suppression of the electron and hole spin relaxation caused by the hyperfine interaction with atomic nuclei [11–13]. Organic semiconductors are nonmagnetic materials, so at small magnetic fields the average electron and nuclear spin polarizations are negligible. However, there are unavoidable nuclear spin fluctuations which create a stochastic Overhauser field for the electrons. Due to this, in a zero external magnetic field, the electron spin precesses with random frequency between the hops, which results in the spin relaxation [14,15]. By contrast, in the strong magnetic field, the electron spin precession frequency is equal to Larmor frequency, which is the same for all hopping sites,

so the spin relaxation gets suppressed [16]. Recently, some of us have shown that OMAR can be related to the nonequilibrium electron spin correlations [17,18], which appear due to the applied voltage. The relaxation of these correlations leads to OMAR.

Nevertheless, to date there is no unambiguous experimental proof of the nuclear origin of OMAR. At the same time, the spin-orbit interaction can play an important role in the hopping conductivity regime [19–21]. In Refs. [22,23] it was suggested as an origin of OMAR. Some other alternatives have been also suggested [24]. Therefore it is desirable to propose an experiment which can evidence the role of nuclear spins. In this paper we propose measurement of the current noise spectra in mesoscopic organic semiconductors. Although the nuclear spins are often assumed to be static [12,18,25–27], their dynamics unavoidably takes place due to the interaction with the electrons. This dynamics is slow and does not change the average electric current. However, it leads to the fluctuations of the current in the mesoscopic samples at small frequencies determined by the nuclear spin dynamics. These fluctuations can be suppressed by the external magnetic field similar to OMAR, which allows one to separate them from shot and  $1/f$  noises. In this paper we calculate the current noise spectrum and demonstrate that its measurement will allow one to prove experimentally the importance of the hyperfine interaction in OMAR.

The paper is organized as follows. In the next section we describe the two alternative microscopic mechanisms of OMAR and establish for them a common relation between current and nuclear spin correlations. Then in Sec. III we calculate the current noise spectra in mesoscopic organic semiconductors. In Sec. IV we discuss the limits of applicability of our theory and summarize our findings.

**II. RELATION BETWEEN NUCLEAR SPINS AND RESISTIVITY**

OMAR is caused by the dependence of the resistivity on the spin relaxation time. Microscopically, there are two main

\* avshumilin@mail.ioffe.ru

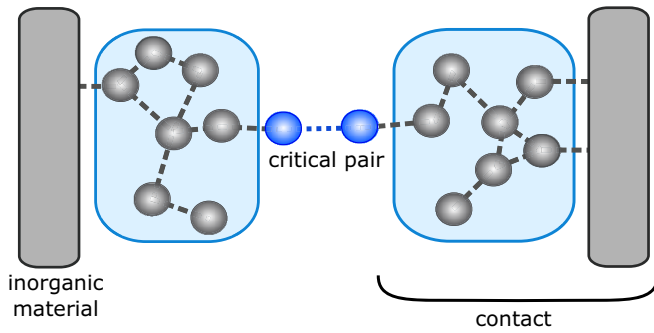


FIG. 1. The structure of a mesoscopic sample. Inorganic contacts (gray areas) are connected to the parts of the percolation cluster with relatively high conductivity. Together they represent an effective contact for the critical pair of sites, which controls the conductivity of the organic layer.

mechanisms of this dependence: (i) In the *bipolaron mechanism*, it is assumed that each hopping site can be occupied by two electrons or two holes if they are in the singlet state only due to the strong exchange interaction [12]. (ii) The *electron-hole mechanism* is based on the spin-dependent recombination of electrons and holes [11]. Its rate is assumed to be different for the singlet and triplet states of the electron-hole pair. In both mechanisms it is necessary to take into account correlations between spins of the charge carriers to describe OMAR [17,18,28]. Below we present the common model for the description of the conductivity in the mesoscopic sample and then calculate the electric current for the electron-hole and bipolaron mechanisms of OMAR. We focus our discussion on the mesoscopic samples because the current noise in them is the strongest.

The distribution of the hopping rates in organic semiconductors is exponentially broad due to the following reasons: (i) The overlap integrals between neighboring hopping sites differ by several orders of magnitude [29]. (ii) The typical width of the distribution of site energies in organic semiconductors is 0.1 eV, which is much larger than the thermal energy at room temperature. Therefore the transport in organic semiconductors can be described by the percolation theory [8]. It stands that the so-called percolation cluster carries most of the current. The cluster consists of pairs of sites with hopping rates faster than or comparable with the critical hopping rate. Most of the hops in the percolation cluster are much faster than the critical rate and are not essential for the calculation of conductivity. The conductivity is controlled by the rare “critical” pairs of sites in the percolation cluster where the hopping rates are comparable to the critical rate. The typical distance between these pairs is called a correlation length of the percolation cluster  $L_c$ . If the size of a sample of organic semiconductor  $L$  is smaller than  $L_c$ , its conductivity is controlled by a single critical pair of sites. In this case the current noise in the sample is the strongest. Note that the mesoscopic sample can still contain a large number of hopping sites, because  $L_c$  is much larger than the typical distance of a single hop [8].

The structure of a mesoscopic sample is shown in Fig. 1. The inorganic contacts are connected to the parts of the percolation cluster with relatively high conductivity. These

parts of the percolation cluster can be considered as parts of the contacts for the critical pair of sites, which controls the conductivity of the sample. The local chemical potentials are formed in these parts of the percolation cluster. In reality they can differ from the chemical potentials in inorganic contacts due to the carrier injection. The overall situation as well as the underlying physics is similar to the double quantum dot system [30,31].

To describe the effect of the nuclear spins on the current, the correlations of electron and hole spin directions should be taken into account. For many charge carriers, there are extremely many correlations. The effect of different spin correlations was studied in detail in Ref. [18] for the bipolaron mechanism of OMAR in close-to-equilibrium conditions. It was found that in the materials where the shape of OMAR is close to Lorentzian [10], it is enough to take into account the correlations between the spins in the closest pairs of sites only. We adopt this approximation and consider the spin correlations in the critical pair of sites only. We assume that the occupation numbers and the spin directions at the sites in the organic parts of the contacts are not correlated with occupation numbers and spins at the critical pair and between themselves. The averaged product of occupation numbers is equal to the product of averaged occupation numbers when the correlations are neglected. The averaged products of spin components are equal to zero without the correlations, because we consider organic semiconductors at high enough temperature.

The spins of electrons and holes in the critical pair of sites interact with atomic nuclei. Typical hopping sites (molecular orbitals) contain dozens of nuclear spins. For example, the molecule of  $\text{Alq}_3$  contains 18 hydrogen atoms with nuclear spins of  $1/2$ , three nitrogen atoms with spins of 1, and one aluminum atom with spin of  $5/2$ . As a result, a single electron spin can interact with  $N$  nuclear spins at each hopping site, where  $N$  is large. Typically, it is assumed to be infinite so that the nuclear spin dynamics due to the hyperfine interaction can be neglected [12,32–35]. In this work, however, we account for the slow nuclear spin dynamics at the timescale  $\propto N$  caused by the electron Knight field.

The distribution of the coupling constants strongly depends on the electron wave function [36]. In this work we abstain from the description of the complex structure of the hopping sites and imagine them as some “spinosaurus” carrying nuclear spins, see Fig. 2. The electrons and holes hop over the backs of the spinosaurus and uniformly interact with the nuclear spins, which is usually called a box model. For this oversimplified model the compact expressions for the nuclear spin dynamics were derived in Ref. [37]. They will be used below to describe the electric current fluctuations. The applicability of this model to the general central spin problem is discussed also in Ref. [37].

Typically the charge-carrier wave functions in organic semiconductors are composed of the  $\pi$ -type orbitals. However, the hyperfine interaction is usually dominated by the admixture of the  $s$ -type orbitals [14,35], so we assume it to be isotropic.

We also assume that the charge-carrier spins at the different sites of the critical pair interact with the different nuclei. At each site the electron spin precession frequency  $\Omega_e$  is

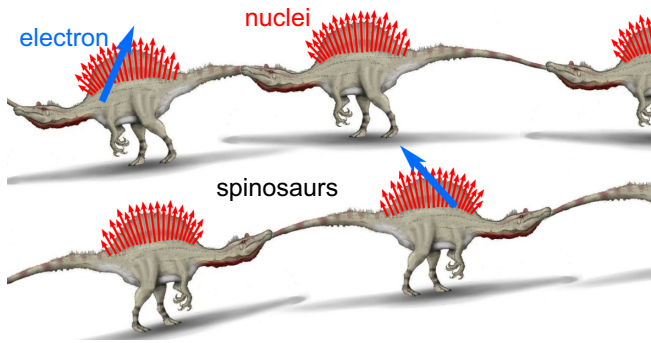


FIG. 2. Impression of the electron spin (blue arrow) hopping between complex organic molecules (spinosaurus), which carry nuclear spins (red arrows). The orientation of nuclear spins in the equilibrium is random.

composed of the spin precession frequency in the external magnetic field  $\Omega_B$  and the precession frequency in the fluctuation of the nuclear field  $\Omega_N$ :

$$\Omega_e = \Omega_B + \Omega_N. \quad (1)$$

The dynamics of  $\Omega_N$  is much slower than the typical hopping rates, so we neglect this dynamics for the description of the average conductivity. The distribution of the spin precession frequencies is described by the function

$$\mathcal{F}(\Omega_N) = \frac{1}{(\sqrt{\pi}\delta)^3} \exp(-\Omega_N^2/\delta^2), \quad (2)$$

where parameter  $\delta$  describes the dispersion.

An important feature of organic semiconductors is the vanishing concentration of the resident charge carriers in the equilibrium. The electrons are injected from the contacts, so the usual linear response theory is typically unacceptable for organic semiconductors [38]. For this reason we consider the nonlinear regime of the conductivity. We will show below that for the both mechanisms of OMAR, the current has the form

$$J = J_0 + J_1 \cos^2(\theta_{12}). \quad (3)$$

Here  $J_0$  is the contribution, that is independent of the nuclear spins,  $\theta_{12}$  is the angle between the spin precession frequencies  $\Omega_e$  at the critical pair of sites, and  $J_1$  describes the amplitude of the contribution, that is sensitive to the magnetic field. The microscopic expressions for  $J_0$  and  $J_1$  will be obtained below for the nonlinear conductivity regime. The fluctuations of  $\theta_{12}$  lead to the electric current noise.

Using the distribution function (2) we find the average electric current

$$\langle J \rangle = J_0 + J_1 \langle \cos^2(\theta_{12}) \rangle, \quad (4)$$

where

$$\langle \cos^2(\theta_{12}) \rangle = \frac{1}{3} + \frac{3}{2} \left( \frac{\delta}{\Omega_B} \right)^6 \left[ \frac{2}{3} \left( \frac{\Omega_B}{\delta} \right)^3 - \frac{\Omega_B}{\delta} + 3D \left( \frac{\Omega_B}{\delta} \right) \right]^2, \quad (5)$$

with  $D(x) = \exp(-x^2) \int_0^x \exp(y^2) dy$  being the Dawson integral. This expression is shown in Fig. 3. One can see that the external magnetic field of the order of  $\delta$  changes the electric current by the value of about  $J_1$ . Typically, in the experiments

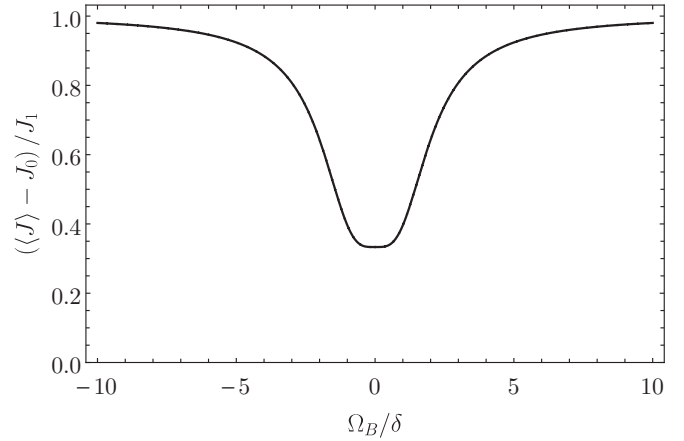


FIG. 3. The magnetic-field-dependent contribution to the electric current [ $\langle \cos^2(\theta_{12}) \rangle$ ] as a function of the Larmor precession frequency calculated after Eq. (5).

$J_1/J_0 \sim 0.1$  [10]. OMAR takes place in the fields of the order of a few millitesla [39–41], which corresponds to  $\delta \sim 1 \text{ ns}^{-1}$ .

### A. Bipolaron mechanism

The bipolaron mechanism is related to the possibility of double occupation of a single hopping site by two electrons or two holes in the singlet spin state only. To be specific, we will consider the electrons. Since the electron spin is conserved during the hop, the hopping from a singly occupied site to another singly occupied site is possible only when the spins are in the singlet state. The detailed theory of bipolaron mechanism of OMAR including all the possible spin correlations in close-to-equilibrium conditions, was developed in Ref. [18]. This theory involves two types of hopping sites: *A*-type sites, which are never doubly occupied, and *B*-type sites, which can be doubly occupied but never lose the last electron. In this work we adopt this model to consider a mesoscopic sample where the critical pair consists of *A* and *B* sites (Fig. 4). In contrast to the previous model, we do not assume the system to be close to the equilibrium.

The dynamics of the spin correlations in the critical pair is described by the following equation [18]:

$$\frac{d \overline{s_A^\alpha s_B^\beta}}{dt} = -R_{\alpha\beta:\alpha'\beta'} \overline{s_A^{\alpha'} s_B^{\beta'}} - \frac{J_{AB}}{4e} \delta_{\alpha\beta}. \quad (6)$$

Here the sum over the repeating indices is assumed,  $\overline{s_A^\alpha s_B^\beta}$  is the quantum-mechanical average of the product of components of

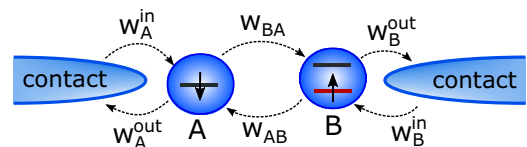


FIG. 4. Illustration of the bipolaron mechanism of OMAR. The *B* site is always occupied with an electron, which is indicated by the red energy level. The dashed arrows with the labels show the possible hops and the corresponding rates.

spins at sites  $A$  and  $B$ ,

$$J_{AB} = 2eW_{AB}\bar{n}_B - eW_{BA}\frac{\bar{n}_A - 4s_A^{\alpha\alpha}s_B^{\alpha\alpha}}{2} \quad (7)$$

is the current between  $A$  and  $B$  sites, with  $\bar{n}_A$  and  $\bar{n}_B$  being the average probabilities of single and double occupation of these sites, respectively, and  $e$  is the electron charge. The notations of the hopping rates are introduced in Fig. 4. Due to the small concentration of electrons in organic semiconductors we take  $\bar{n}_A\bar{n}_B = 0$ .

The last term in Eq. (6) describes the generation of the spin correlations due to the spin-dependent hopping. Another term describes the dynamics and relaxation of the spin correlations due to the hyperfine interaction and hopping:

$$R_{\alpha\beta;\alpha'\beta'} = W_A^{\text{out}}\delta_{\alpha\alpha'}\delta_{\beta\beta'} + \frac{W_{BA}}{2}(\delta_{\alpha\alpha'}\delta_{\beta\beta'} - \delta_{\alpha\beta'}\delta_{\beta\alpha'}) - (\epsilon_{\alpha\gamma\alpha'}\delta_{\beta\beta'}\Omega_{e,\gamma}^{(A)} + \epsilon_{\beta\gamma\beta'}\delta_{\alpha\alpha'}\Omega_{e,\gamma}^{(B)}). \quad (8)$$

Here  $\Omega_e^{(A)}$  and  $\Omega_e^{(B)}$  are the spin precession frequencies at the corresponding sites given by Eq. (1) and  $\epsilon_{\alpha\beta\gamma}$  is the Levi-Civita symbol.

In Appendix A we obtain the current in the form

$$J_{AB} = \frac{2\bar{n}_B W_{AB} - \bar{n}_A W_{BA}/2}{1 + W_{BA}\mathcal{T}_s^{(AB)}/2}, \quad (9)$$

where

$$\mathcal{T}_s = (R^{-1})_{\alpha\alpha';\alpha'\alpha'} \quad (10)$$

is the effective relaxation time of the spin correlations. In the steady state, the current  $J_{AB}$  flows also to and from the contacts, so it can be calculated from the kinetic equations

$$J_{AB} = e\bar{n}_A W_A^{\text{out}} - eW_A^{\text{in}}(1 - \bar{n}_A), \quad (11a)$$

$$J_{AB} = eW_B^{\text{in}}(1 - \bar{n}_B) - e\bar{n}_B W_B^{\text{out}}. \quad (11b)$$

These expressions represent the current through the contacts attached to sites  $A$  and  $B$ , respectively. From these relations we find the occupancies  $\bar{n}_A$ ,  $\bar{n}_B$  and calculate the current for the given orientation of the nuclear spins imprinted in  $\mathcal{T}_s^{(AB)}$ .

By the definition of the critical pair,  $W_A^{\text{out}} \gg W_{BA}$ . Moreover, to simplify the analysis, we consider the limit  $\Omega_e^{(A),(B)} \gg W_A^{\text{out}}$ . In this case we obtain

$$\mathcal{T}_s = \frac{1}{W_A^{\text{out}}} \cos^2(\theta_{AB}), \quad (12)$$

where  $\theta_{AB}$  is the angle between  $\Omega_e^{(A)}$  and  $\Omega_e^{(B)}$ . In this limit the contributions to the total current in Eq. (3) are

$$J_0 = e \frac{4W_B^{\text{in}}W_{AB}W_A^{\text{out}} - W_A^{\text{in}}W_{BA}W_B^{\text{out}}}{4W_{AB}W_A^{\text{out}} + 2W_A^{\text{out}}W_B^{\text{out}} + W_{BA}W_B^{\text{out}}}, \quad (13a)$$

$$J_1 = e \frac{W_{BA}W_B^{\text{out}}(W_A^{\text{in}}W_{BA}W_B^{\text{out}} - 4W_B^{\text{in}}W_{AB}W_A^{\text{out}})}{[4W_{AB}W_A^{\text{out}} + (2W_A^{\text{out}} + W_{BA})W_B^{\text{out}}]^2}, \quad (13b)$$

and  $\theta_{12} = \theta_{AB}$ .

## B. Electron-hole mechanism

The electron-hole mechanism of OMAR involves the ambipolar transport. In this case, each molecule provides two

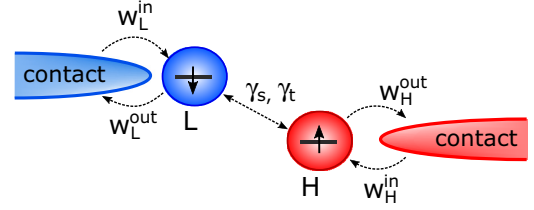


FIG. 5. Illustration of the electron-hole mechanism of OMAR. LUMO sites (blue) and HOMO sites (red) can be occupied by electrons and holes, respectively. The arrows and labels show the possible hops and the corresponding rates.

hopping sites. Its highest occupied molecular orbital (HOMO) and lowest unoccupied molecular orbital (LUMO) represent the hopping sites for holes and electrons, respectively. Electrons and holes in organic semiconductors usually have spin 1/2 due to the weak spin-orbit interaction. In the electron-hole mechanism, the relation between current and charge carrier spin relaxation is provided by the spin-dependent recombination of electron-hole pairs.

We assume that the critical pair in the mesoscopic sample is represented by LUMO site  $L$  and HOMO site  $H$  (Fig. 5). In particular, this means that an electron-hole pair (or an exciplet) cannot move and always interacts with the same nuclei, in contrast with Ref. [42]. This regime is expected to be realized for the strong energy disorder with the short correlation length. The current in this pair  $J_{LH}$  flows due to the recombination of electrons and holes. It has the form

$$J_{LH} = e\gamma_s \left( \frac{\bar{n}_L \bar{p}_H - 4s_L^{\alpha\alpha}s_H^{\alpha\alpha}}{4} \right) + e\gamma_t \left( \frac{3\bar{n}_L \bar{p}_H + 4s_L^{\alpha\alpha}s_H^{\alpha\alpha}}{4} \right), \quad (14)$$

where  $\gamma_s$  and  $\gamma_t$  are the electron-hole recombination rates for the singlet and triplet states, respectively, and the other notations are the same as in the previous section except for the substitution of the indices  $L, H$  for  $A, B$ . We denote the  $H$  site occupancy as  $p_H$  to show that it is related to a hole. The current depends on the spin correlations, when  $\gamma_s \neq \gamma_t$ .

To derive the master equation for the spin correlations, we assume that the singlet and triplet recombination processes are independent. In this case we obtain

$$\frac{ds_L^{\alpha\alpha}s_H^{\beta\beta}}{dt} = -R_{\alpha\beta;\alpha'\beta'} \overline{s_L^{\alpha\alpha}s_H^{\beta\beta}} + (\gamma_s - \gamma_t) \frac{\bar{n}_L \bar{p}_H - 4s_L^{\alpha\alpha}s_H^{\beta\beta}}{16} \delta_{\alpha\beta}, \quad (15)$$

where the relaxation matrix is given by

$$R_{\alpha\beta;\alpha'\beta'} = (W_L^{\text{out}} + W_H^{\text{out}} + \gamma_t)\delta_{\alpha\alpha'}\delta_{\beta\beta'} + \gamma_s(\delta_{\alpha\alpha'}\delta_{\beta\beta'} - \delta_{\alpha\beta'}\delta_{\beta\alpha'}) - \epsilon_{\alpha\gamma\alpha'}\delta_{\beta\beta'}\Omega_{e,\gamma}^{(L)} - \epsilon_{\beta\gamma\beta'}\delta_{\alpha\alpha'}\Omega_{e,\gamma}^{(H)}. \quad (16)$$

Here  $\Omega_e^{(L)}$  and  $\Omega_e^{(H)}$  are the spin precession frequencies of the electron at site  $L$  and hole at site  $H$ , respectively, and the hopping rates are introduced in Fig. 5.

For the steady state we show in Appendix B that the current is given by

$$J_{LH} = e\bar{n}_L \bar{p}_H \tilde{\gamma}, \quad (17)$$

where

$$\tilde{\gamma} = \gamma_t + \frac{\gamma_s - \gamma_t}{4 + \mathcal{T}_s(\gamma_s - \gamma_t)} \quad (18)$$

is the effective electron-hole recombination rate depending on the orientations of the nuclear spins through the effective relaxation time given by Eq. (10). From kinetic equations for contacts, the current also equals to

$$J_{LH} = e(1 - \bar{n}_L)W_L^{\text{in}} - e\bar{n}_L W_L^{\text{out}}, \quad (19a)$$

$$J_{LH} = eW_H^{\text{in}}(1 - \bar{p}_H) - eW_H^{\text{out}}\bar{p}_H. \quad (19b)$$

To find the current, these equations should be solved together with the kinetic equation for the correlation of occupancies:

$$(\tilde{W}_L + \tilde{W}_H + \tilde{\gamma})\bar{n}_L\bar{p}_H = W_L^{\text{in}}\bar{p}_H + W_H^{\text{in}}\bar{n}_L, \quad (20)$$

where  $\tilde{W}_L = W_L^{\text{in}} + W_L^{\text{out}}$  and  $\tilde{W}_H = W_H^{\text{in}} + W_H^{\text{out}}$ . This set of equations allows one to find the electric current for the given hopping rates and nuclear spin orientations.

When the electron spin precession is fast as compared with the hopping and recombination,  $\Omega_e^{(L)}, \Omega_e^{(H)} \gg W_L^{\text{out}} + W_H^{\text{out}} + \gamma_t \gg \gamma_s$ , we obtain

$$\mathcal{T}_s = \frac{\cos^2(\theta_{LH})}{W_L^{\text{out}} + W_H^{\text{out}} + \gamma_t}, \quad (21)$$

where  $\theta_{LH}$  is the angle between  $\Omega_e^{(L)}$  and  $\Omega_e^{(H)}$ . Thus we can find the current for arbitrary  $\tilde{\gamma}$  and, therefore, for arbitrary nuclear spin directions. In this limit, the current is again given by Eq. (3), where

$$J_0 = \frac{e\tilde{\gamma}_0 W_L^{\text{in}} W_H^{\text{in}} (\tilde{W}_L + \tilde{W}_H)}{\tilde{\gamma}_0 (W_L^{\text{in}} \tilde{W}_L + W_H^{\text{in}} \tilde{W}_H) + \tilde{W}_L \tilde{W}_H (\tilde{\gamma}_0 + \tilde{W}_L + \tilde{W}_H)}, \quad (22a)$$

$$J_1 = \frac{(\gamma_s - \gamma_t)^2}{16(W_L^{\text{out}} + W_H^{\text{out}} + \gamma_t)} \times \frac{e\tilde{\gamma}_0 W_L^{\text{in}} W_H^{\text{in}} \tilde{W}_L \tilde{W}_H (\tilde{W}_L + \tilde{W}_H)^2}{[\tilde{\gamma}_0 (W_L^{\text{in}} \tilde{W}_L + W_H^{\text{in}} \tilde{W}_H) + \tilde{W}_L \tilde{W}_H (\tilde{\gamma}_0 + \tilde{W}_L + \tilde{W}_H)]^2}, \quad (22b)$$

and  $\theta_{12} = \theta_{LH}$  for the case of the electron-hole mechanism.

To summarize this section, we have calculated the electric current in the mesoscopic organic semiconductor without assumption of close-to-equilibrium conditions for the two mechanisms of OMAR. The current has the form of Eq. (3), and it is determined by the squared cosine of the angle between the spin precession frequencies in the critical pair of sites. In the next section we use this result to describe the electric current fluctuations.

### III. ELECTRIC CURRENT NOISE

Dynamics of the nuclear spins lead to the current fluctuations in mesoscopic organic semiconductors. The absolute value of the current fluctuations in mesoscopic samples have the same order as OMAR, which can reach 10% [10]. The current noise spectrum is given by

$$(\delta J^2)_\omega = \int_{-\infty}^{\infty} \langle \delta J(0) \delta J(t) \rangle e^{i\omega t} dt, \quad (23)$$

where  $\delta J(t) = J(t) - \langle J \rangle$  is the current fluctuation, and angular brackets denote the statistical averaging over the nuclear spin orientations and hops. For the bipolaron and electron-hole mechanisms,  $J$  should be replaced with  $J_{AB}$  and  $J_{LH}$ , respectively. We will study the current noise related to the nuclear spin dynamics only, and the other contributions will be briefly discussed in Sec. IV.

For simplicity, we assume that the electron hopping is much faster than the nuclear spin precession and electron spin relaxation, which is much faster than the nuclear spin relaxation. Under these assumptions, the current noise can be described in a unified way for the bipolaron and electron-hole mechanisms. We will use the notations for the bipolaron mechanism. Unless it is explicitly stated, for the electron-hole mechanism the upper indices  $A$  and  $B$  should be replaced with the indices  $L$  and  $H$ .

As mentioned above, for each hopping site we use the box model of the hyperfine interaction, which was solved in Ref. [37] for many nuclear spins. The frequency  $\Omega_N$  is related to the total nuclear spin  $\mathbf{I}$  as  $\Omega_N = A\mathbf{I}/\hbar$ , where  $A$  is the hyperfine coupling constant. The nuclear spin dynamics,  $\mathbf{I}(t)$ , is described by the kinetic equation for the two-component probability distribution function  $f_\pm(t, \mathbf{I})$ :

$$\frac{\partial f_\pm}{\partial t} + \nabla \left[ \left( \boldsymbol{\omega}_n^\pm \times \mathbf{I} - \frac{\mathbf{I}}{\tau_s^n} \right) f_\pm \right] + D \Delta f_\pm + \frac{f_\pm - f_\mp}{\tau_s^e} = 0. \quad (24)$$

Here the two components with the subscript  $\pm$  correspond to the electron spin parallel and antiparallel to the direction of  $\Omega_e$  [Eq. (1)], which is a good quantization axis at the timescale of the nuclear spin dynamics;  $\nabla = \partial/\partial \mathbf{I}$ ;  $\Delta = \nabla^2$ ;  $\tau_s^{n,e}$  are the phenomenological nuclear and electron spin relaxation times unrelated with the hyperfine interaction, respectively; and  $D = (\hbar\delta/A)^2/(2\tau_s^n)$  is the effective diffusion coefficient. The nuclear spin dynamics mainly represents the precession with the frequency

$$\boldsymbol{\omega}_n^\pm = \pm \omega_e \frac{\boldsymbol{\Omega}_B}{\Omega_e} + \boldsymbol{\omega}_B, \quad (25)$$

where  $\omega_e = A/(2\hbar)$  is the nuclear spin precession frequency in the Knight field of a completely spin polarized electron, and  $\boldsymbol{\omega}_B$  is the nuclear spin precession frequency in the external magnetic field. To give an estimate we note that for  $N$  nuclei  $\omega_e \propto \delta/\sqrt{N}$ . Thus for  $N = 100$  we obtain  $\omega_e \sim 0.1 \text{ ns}^{-1}$ . The phenomenological spin relaxation time  $\tau_s^n$  can be related with the dipole-dipole interactions or quadrupole interaction [36], and we expect it to be of the order of  $1 \mu\text{s}$ . The steady state solution of Eq. (24) has the form  $f_\pm = f^{(0)}(\mathbf{I})$ , where

$$f^{(0)}(\mathbf{I}) = \frac{1}{2} \left( \frac{A}{\sqrt{\pi} \hbar \delta} \right)^3 \exp \left[ - \left( \frac{A\mathbf{I}}{\hbar \delta} \right)^2 \right], \quad (26)$$

in agreement with Eq. (2).

In Appendix C we show that the current from Eq. (3) can be written as

$$J_{AB} = \mathcal{J}_0 + \mathcal{J}_1 \cos(\varphi) + \mathcal{J}_2 \cos(2\varphi), \quad (27)$$

where  $\varphi$  is the polar angle between  $\mathbf{I}^{(A)}$  and  $\mathbf{I}^{(B)}$ , and

$$\mathcal{J}_0 = J_0 + J_1 \times \frac{(O_b + I_z^{(A)})^2 (O_b + I_z^{(B)})^2 + (I_\perp^{(A)} I_\perp^{(B)})^2 / 2}{|\mathbf{O}_b + \mathbf{I}^{(A)}|^2 |\mathbf{O}_b + \mathbf{I}^{(B)}|^2}, \quad (28a)$$

$$\mathcal{J}_1 = J_1 \frac{2(O_b + I_z^{(A)})(O_b + I_z^{(B)}) I_\perp^{(A)} I_\perp^{(B)}}{|\mathbf{O}_b + \mathbf{I}^{(A)}|^2 |\mathbf{O}_b + \mathbf{I}^{(B)}|^2}, \quad (28b)$$

$$\mathcal{J}_2 = J_1 \frac{(I_\perp^{(A)} I_\perp^{(B)})^2}{2|\mathbf{O}_b + \mathbf{I}^{(A)}|^2 |\mathbf{O}_b + \mathbf{I}^{(B)}|^2}. \quad (28c)$$

Here  $J_0$  and  $J_1$  are given by Eqs. (13) or Eqs. (22), depending on the mechanism,  $O_b = \hbar\Omega_B/A$  is a dimensionless frequency of the electron spin precession in the external magnetic field directed along  $z$  axis, and  $I_\perp^{(A,B)}$  are the absolute values of the spin components in the  $(xy)$  plane.

The three contributions in Eq. (27) lead to the three independent contributions to the current noise spectrum. We assume that the typical nuclear spin precession frequency  $\omega_e$  and the electron spin relaxation rate  $1/\tau_s^e$  are much larger than the nuclear spin relaxation rate  $1/\tau_s^n$ . In this case, the contribution related to  $\mathcal{J}_0$  represents the low-frequency noise at frequencies of the order of  $1/\tau_s^n$ . The two other terms give rise to the high-frequency noise at the frequencies of the order of  $\omega_e$ . It is caused by the nuclear spin precession in the Knight field. Accordingly, the current noise spectrum can be written as

$$(\delta J^2)_\omega = (\delta J^2)_\omega^{(HF)} + (\delta J^2)_\omega^{(LF)}. \quad (29)$$

Below we separately calculate these two contributions.

### A. High-frequency noise

The reason for the high-frequency noise is the precession of the nuclear spins in the Knight field of the electron or hole localized at the given site. This precession takes place only when the site is singly occupied. At unoccupied and doubly occupied sites there is no Knight field.

For the bipolaron mechanism, we assume that the number of the current-carrying electrons is much smaller than the number of hopping sites, so their effect on the nuclear spins can be neglected. Nevertheless, one electron is always present at site  $B$  in the critical pair. It leads to the precession of the total nuclear spin  $\mathbf{I}^{(B)}$  at the  $B$  site around the magnetic field. In the same time, the nuclear spin  $\mathbf{I}^{(A)}$  at the  $A$  site is static neglecting the slow nuclear spin relaxation.

In the electron-hole mechanism there are no resident charge carriers at sites  $L$  and  $H$ . Nevertheless, the high-frequency current noise takes place if one of the sites  $L$  or  $H$  acts as a trap for the charge carriers. It means that this site is almost always occupied. For site  $H$  the condition of being a trap is  $W_H^{\text{in}} \gg \tilde{\gamma}, \omega_n, W_H^{\text{out}}$ . This condition ensures that site  $H$  gets occupied almost immediately after losing its hole due to the recombination or hopping to the contact. In this case, it represents an analog of the  $B$  site. The other site should be analogous to the  $A$  site in the bipolaron mechanism, and its occupation probability should be small. Under these assumptions the high-frequency noise

in the bipolaron and electron-hole mechanism is the same. To be specific, we will use the notations of the bipolaron mechanism.

During the transmission of an electron through the critical pair, the two electrons form a singlet spin state at the  $B$  site. So after the fast transmission, the electron at the  $B$  site becomes depolarized. The corresponding spin relaxation rate is

$$\frac{1}{\tau_s^e} = W_B^{\text{in}} + W_A^{\text{in}} \frac{W_{BA}}{W_{BA} + 2W_A^{\text{out}}}. \quad (30)$$

It defines the phenomenological spin relaxation time for the  $B$  site. In the case of the electron-hole mechanism the spin relaxation time equals  $1/W_H^{\text{out}}$  or  $1/W_L^{\text{out}}$  when the  $H$  or  $L$  site represents a trap, respectively.

At timescales much shorter than the nuclear spin relaxation time, the nuclear spin dynamics can be simply described by the two coupled Bloch equations:

$$\frac{d\mathbf{I}^\pm}{dt} = \boldsymbol{\omega}_n^\pm \times \mathbf{I}^\pm + \frac{\mathbf{I}^\mp - \mathbf{I}^\pm}{2\tau_s^e}, \quad (31)$$

where

$$\mathbf{I}_\pm = \int f_\pm(t, \mathbf{I}) d\mathbf{I} \quad (32)$$

represents the average nuclear spins in the corresponding electron spin subspaces. Moreover, it is convenient to use the coordinate frame rotating with the frequency  $\omega_B$ , because the electric current depends only on the angle between nuclear spins at the critical pair of sites. We assume that  $\omega_B$  at these sites is the same. As a result, one can neglect the nuclear spin dynamics at the  $A$  site along with the frequency  $\omega_B$  at the  $B$  site.

Let us consider the current noise related to  $\mathcal{J}_1$  in Eq. (27). It is useful to introduce the correlation functions  $c_{\sigma, \sigma'} = \langle e^{i\varphi(t)} \cos \varphi(0) \rangle_{\sigma, \sigma'}$ , where  $\sigma, \sigma' = \pm$  correspond to the orientation of the electron spin at the  $B$  site parallel or antiparallel to the  $z$  axis at the time moments  $t$  and  $0$ , respectively. To calculate the average, the expression in brackets should be multiplied by the corresponding spin projector operators at times  $0$  and  $t$ . The correlators obey the equations (at  $t > 0$ )

$$\frac{d}{dt} c_{\pm, \sigma} = \pm i\omega_n^{(B)} c_{\pm, \sigma} + \frac{c_{\mp, \sigma} - c_{\pm, \sigma}}{2\tau_s^e}, \quad (33)$$

according to Eq. (31). The initial conditions are  $c_{\sigma, \sigma'}(0) = \delta_{\sigma, \sigma'}/4$ . From the solution of these equations, the contribution to the current noise can be obtained as

$$\mathcal{J}_1^2 \sum_{\sigma, \sigma'} \int_{-\infty}^{\infty} \text{Re} [c_{\sigma, \sigma'}(t)] e^{i\omega t} dt. \quad (34)$$

In the same way we obtain the contribution related to  $\mathcal{J}_2$ . The total high-frequency current noise spectrum

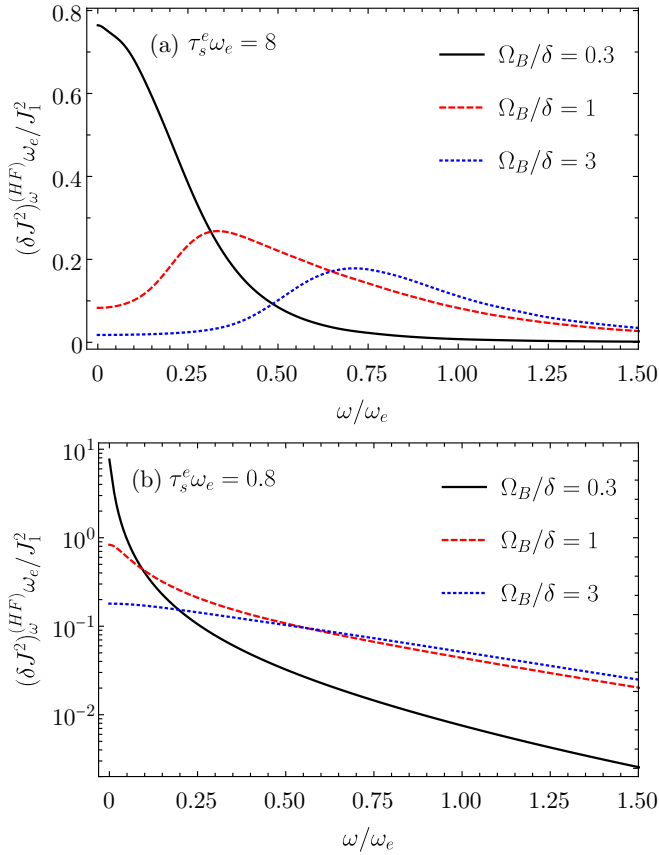


FIG. 6. The high-frequency current noise spectra calculated after Eq. (35) for the different strength of the magnetic field and different spin relaxation times, as indicated in the plots.

reads

$$(\delta J^2)_\omega^{(HF)} = \left\langle \mathcal{J}_1^2 \frac{\tau_s^e (\omega_n^{(B)})^2}{\omega^2 + (\tau_s^e)^2 [\omega^2 - (\omega_n^{(B)})^2]^2} + \mathcal{J}_2^2 \frac{4\tau_s^e (\omega_n^{(B)})^2}{\omega^2 + (\tau_s^e)^2 [\omega^2 - 4(\omega_n^{(B)})^2]^2} \right\rangle, \quad (35)$$

where the angular brackets denote the averaging over the initial nuclear fields distribution only. We perform it numerically. Note that the ratio  $\mathcal{J}_2/\mathcal{J}_1$  does not depend on the hopping rates because both  $\mathcal{J}_1$  and  $\mathcal{J}_2$  are proportional to  $J_1$ , so the shape of the spectrum depends on the hopping rates through  $\tau_s^e$  only.

The high-frequency contribution to the current noise spectrum is shown in Fig. 6. In the limit  $\tau_s^e \gg 1/\omega_e$ , the shape of the spectrum does not depend on the hopping rates. This limit is illustrated in panel (a). The spectrum consists of a single asymmetric peak, which shifts to higher frequencies with increase of the magnetic field. Its central frequency saturates at  $\omega = \omega_e$  in high fields. The additional peak at the frequency  $2\omega_e$ , which can be expected from Eq. (35), is very small and cannot be clearly seen. The current noise intensity decreases with increase of the magnetic field. This is caused by the saturation of OMAR in large fields, when the current becomes independent of the orientations of the nuclear spins. The short electron spin relaxation time

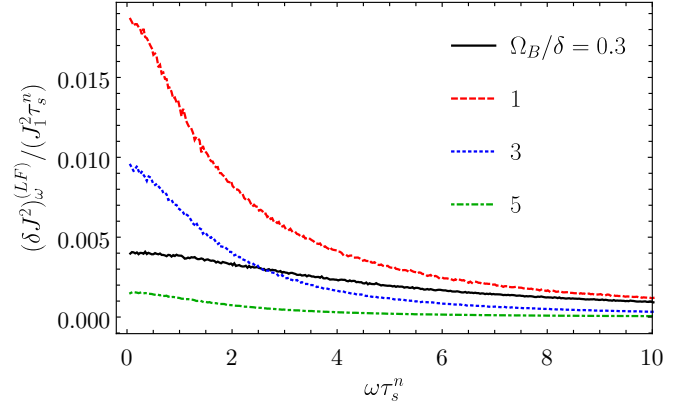


FIG. 7. Low-frequency current noise spectrum simulated numerically for the different magnetic fields.

$\tau_s^e \lesssim 1/\omega_e$  leads to the smearing of the noise spectrum, as shown in Fig. 6(b).

### B. Low-frequency noise

The low-frequency noise is related to the nuclear spin components along the magnetic field, because they are conserved during the spin precession. Their dynamics is caused by the nuclear spin relaxation and leads to the current noise at the frequencies of the order of  $1/\tau_s^n$ .

The low-frequency noise stems from the contribution  $\mathcal{J}_0$  in Eq. (27), which does not depend on the polar angles of nuclear spins, as it can be seen from Eq. (28a). Therefore this contribution can be described accounting for the diffusion-related part of the kinetic eq. (24) only. It is convenient to solve the diffusion equation using the fictitious Langevin forces (for each site):

$$\frac{d\mathbf{I}}{dt} = \boldsymbol{\xi}(t) - \frac{\mathbf{I}}{\tau_s^n}, \quad (36)$$

with the correlation function

$$\langle \xi_\alpha(t) \xi_\beta(t') \rangle = \frac{1}{\tau_s^n} \left( \frac{\hbar\delta}{A} \right)^2 \delta_{\alpha\beta} \delta(t - t'), \quad (37)$$

where  $\delta_{\alpha\beta}$  is the Kronecker symbol and  $\delta(t)$  is the Dirac  $\delta$  function. As a result, the shape of the low-frequency current noise spectrum does not depend on the electron spin relaxation time and the hopping rates.

We simulated the low-frequency noise numerically, generating  $10^3$  times the random forces for the time intervals  $10^3 \tau_s^n$ . The results of the simulation are shown in Fig. 7. The spectrum always represents a peak at zero frequency with the width of the order of  $1/\tau_s^n$ , which somewhat decreases with increase of the magnetic field.

The amplitude of the low-frequency noise non-monotonously depends on the magnetic field. The area under this component of the spectrum is given by

$$\int_{-\infty}^{\infty} (\delta J^2)_\omega^{(LF)} \frac{d\omega}{2\pi} = \langle \delta \mathcal{J}_0^2 \rangle, \quad (38)$$

where we took into account the fact that the low-frequency noise is produced only by the term  $\mathcal{J}_0$  in Eq. (27). It is

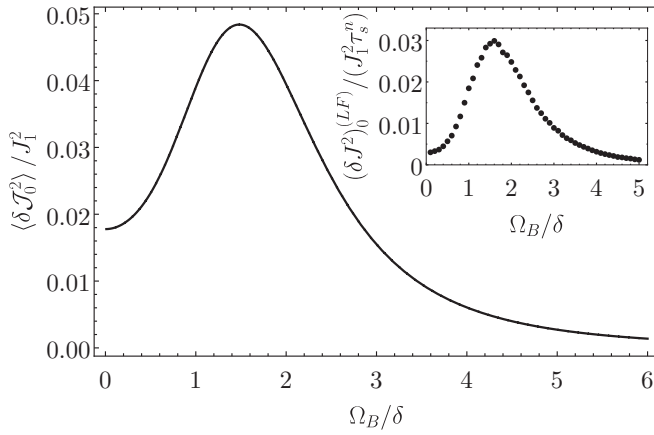


FIG. 8. The low-frequency noise intensity as a function of the magnetic field calculated after Eq. (D5). The inset shows the amplitude of the noise at the zero frequency calculated numerically.

calculated analytically in Appendix D and plotted in Fig. 8 as a function of the magnetic field. The area has a maximum at  $\Omega_B \approx 1.5\delta$  with the maximum value approximately twice its value at zero magnetic field. In addition, the inset in Fig. 8 shows the amplitude of the noise at zero frequency, which has a more pronounced maximum at  $\Omega_B \approx 1.6\delta$ , when it is almost ten times larger than in the zero field.

Qualitatively, these dependencies are nonmonotonous because the low-frequency noise can be viewed as a result of the effective slow variations of the external magnetic field. From Fig. 3 one can see that these variations lead to the largest changes in the current when  $\Omega_B \sim \delta$ , in agreement with Fig. 8.

#### IV. DISCUSSION AND CONCLUSION

In our work we described the current noise in mesoscopic organic semiconductors, where the conductivity is controlled by a single critical pair of sites. In this case the noise is the largest. With increase of the sample size, the percolation cluster becomes more complex and contains more critical pairs [43,44]. The number of critical pairs grows with the sample size  $L$  as  $(L/L_c)^d$ , where  $d = 2, 3$  is the dimension of the sample [8]. As a result, the current noise gets suppressed by the factor  $(L_c/L)^{d/2}$ . For organic semiconductors this regime is known as the “fat percolation,” and the correlation length can be estimated as  $L_c \sim n^{-1/d} [G_{\text{crit}} f(G_{\text{crit}})]^{-\nu}$  [45], where  $G_{\text{crit}}$  is the critical conductivity of the Miller-Abrahams resistor,  $f(G)$  is the distribution of the resistor conductivities,  $n$  is the concentration of the hopping sites, and  $\nu$  is the universal critical index [8].

Crucially, the current noise induced by the nuclear spin fluctuations can be separated from the other sources of noise, such as shot noise, molecular vibrations, and  $1/f$  noise, due to its sensitivity to the external magnetic field. Even if one goes beyond the simplest model of the uniform hyperfine interaction with the nuclei at each site, the noise spectrum would consist of a high-frequency peak and the low-frequency noise [46] (which can be similar to  $1/f$  noise [47,48]). In this case the external magnetic field changes the strength and the shape of these two components, as illustrated in Fig. 8. This

allows one to single them out experimentally. The relevant range of the magnetic fields is the same as for OMAR.

In addition to this, the amplitude and the shape of the low-frequency peak described in Sec. III B can be controlled by the rf field. If it is applied in resonance with  $\omega_B$ , it increases the nuclear spin relaxation rate as [36]

$$\frac{1}{\tau_s^n} = \frac{1}{\tau_s^{n(0)}} + \frac{\tilde{\omega}^2}{2} \frac{\tau_s^{n(0)}}{1 + (\omega_{\text{rf}} - \omega_B)^2 (\tau_s^{n(0)})^2}, \quad (39)$$

where  $\tau_s^{n(0)}$  is the spin relaxation time in the absence of the rf field,  $\tilde{\omega}$  is the nuclear spin precession frequency in the rf field, and  $\omega_{\text{rf}}$  is the carrying frequency of the rf field. Thus application of the rf field leads to the broadening of the low-frequency peak and a decrease of its amplitude. The resonant dependence on  $\omega_{\text{rf}}$  allows for the unambiguous evidence of the role of the nuclei in OMAR.

When OMAR is controlled by the electron-hole mechanism, the electron-hole recombination is often radiative [9,41,42]. This provides a striking opportunity to detect the nuclear spin noise in organic semiconductors by the means of the optical spin noise spectroscopy [49] by measuring the spectrum of the electroluminescence intensity fluctuations.

In conclusion, we calculated the current noise in mesoscopic organic semiconductors caused by the nuclear spin fluctuations. This effect takes place in the samples with pronounced OMAR. The current noise spectrum consists of the two peaks. One is centered at the frequency, which increases with increase of the magnetic field, and the other one is centered at zero frequency. The dependence of the nuclei-induced current noise on the magnetic field as well as on the rf field allows one to separate its contribution to the current noise from the other contributions experimentally.

#### ACKNOWLEDGMENTS

We gratefully acknowledge fruitful discussions with M. M. Glazov and partial funding by RF President Grant No. MK-5158.2021.1.2, Foundation for the Advancement of Theoretical Physics and Mathematics “Basis,” and the Russian Foundation for Basic Research (Grants No. 20-52-16303 and No. 20-32-70048). A.V.S. acknowledges support from the Russian Foundation for Basic Research through Grant No. 19-02-00184.

#### APPENDIX A: DERIVATION OF EQ. (9)

Equation (6) in the steady state yields the spin correlator in the form

$$\overline{s_A^\alpha s_B^\beta} = -(R^{-1})_{\alpha\beta;\alpha'} \frac{J_{AB}}{4e}. \quad (A1)$$

Substituting this expression in Eq. (7) we obtain

$$J_{AB} = 2eW_{AB}\bar{n}_B - e\frac{W_{BA}}{2}\bar{n}_A - \frac{W_{BA}}{2}(R^{-1})_{\alpha\alpha';\alpha'} J_{AB}. \quad (A2)$$

Solution of this linear equation yields Eqs. (9) and (10).

**APPENDIX B: DERIVATION OF EQ. (17)**

Similarly to Appendix A, Eq. (15) in the steady state yields the relation

$$\overline{s_L^\alpha s_H^\beta} = -(R^{-1})_{\alpha\beta;\alpha'\alpha'}(\gamma_s - \gamma_t) \frac{\overline{n_L p_H} - 4\overline{s_L^\gamma s_H^\gamma}}{16}. \quad (\text{B1})$$

In the same time, Eq. (14) can be written as follows:

$$J_{LH} = e\gamma_s \left( \frac{\overline{n_L p_H} - 4\overline{s_L^\alpha s_H^\alpha}}{4} \right) + e\gamma_t \overline{n_L p_H} - e\gamma_t \left( \frac{\overline{n_L p_H} - 4\overline{s_L^\alpha s_H^\alpha}}{4} \right). \quad (\text{B2})$$

From this relation we express the right-hand side of Eq. (B1) as

$$(\gamma_s - \gamma_t) \frac{\overline{n_L p_H} - 4\overline{s_L^\alpha s_H^\alpha}}{16} = \frac{1}{4}(J_{LH} - e\gamma_t \overline{n_L p_H}). \quad (\text{B3})$$

Substituting this in Eq. (B1), we obtain the spin correlator:

$$\overline{s_L^\alpha s_H^\beta} = -(R^{-1})_{\alpha\beta;\alpha'\alpha'} \frac{1}{4}(J_{LH} - e\gamma_t \overline{n_L p_H}). \quad (\text{B4})$$

Substituting it in Eq. (14) and solving the linear equation for  $J_{LH}$  we obtain Eqs. (17) and (18).

**APPENDIX C: DERIVATION OF EQS. (28)**

By the definition of  $\mathbf{O}_b$ ,  $\Omega_e^{(A),(B)} = (A/\hbar)(\mathbf{O}_b + \mathbf{I}^{(A),(B)})$ , so the cosine of the relative angle between  $\Omega_e^{(A)}$  and  $\Omega_e^{(B)}$  is given by

$$\cos \theta_{AB} = \frac{(\mathbf{O}_b + \mathbf{I}^{(A)})(\mathbf{O}_b + \mathbf{I}^{(B)})}{|\mathbf{O}_b + \mathbf{I}^{(A)}||\mathbf{O}_b + \mathbf{I}^{(B)}|}. \quad (\text{C1})$$

Expanding the numerator we obtain

$$\cos \theta_{AB} = \frac{(\mathbf{O}_b + I_z^{(A)})(\mathbf{O}_b + I_z^{(B)})}{|\mathbf{O}_b + \mathbf{I}^{(A)}||\mathbf{O}_b + \mathbf{I}^{(B)}|} + \frac{I_\perp^{(A)} I_\perp^{(B)} \cos \varphi}{|\mathbf{O}_b + \mathbf{I}^{(A)}||\mathbf{O}_b + \mathbf{I}^{(B)}|}. \quad (\text{C2})$$

Further, calculating the square of this expression and taking into account the fact that the denominators do not depend on  $\varphi$  along with the relation  $\cos^2(\varphi) = [1 + \cos(2\varphi)]/2$ , we obtain the coefficients of the decomposition of Eq. (3) in the form of Eq. (28).

**APPENDIX D: INTENSITY OF THE LOW-FREQUENCY CURRENT NOISE**

The low-frequency noise is described by the contribution  $\mathcal{J}_0$  given by Eq. (28a). It can be expressed in terms of the angles  $\theta_A$  and  $\theta_B$  between the  $z$  axis and the frequencies  $\Omega_e^{(A),(B)}$  as follows:

$$\mathcal{J}_0 = J_1 \left[ \cos^2(\theta_A) \cos^2(\theta_B) + \frac{\sin^2(\theta_A) \sin^2(\theta_B)}{2} \right]. \quad (\text{D1})$$

Due to the independence of the two angles the low-frequency current noise correlator takes the form

$$\langle \delta \mathcal{J}_0^2 \rangle = J_1^2 \left[ \frac{9}{4} [\langle \sin^4(\theta_A) \rangle^2 - \langle \sin^2(\theta_A) \rangle^4] - 6 [\langle \sin^4(\theta_A) \rangle \langle \sin^2(\theta_A) \rangle - \langle \sin^2(\theta_A) \rangle^3] + 2 [\langle \sin^4(\theta_A) \rangle - \langle \sin^2(\theta_A) \rangle^2] \right]. \quad (\text{D2})$$

Here the averages can be calculated using Eqs. (1) and (2):

$$\langle \sin^2(\theta_A) \rangle = \frac{\delta^2 \Omega_B - \delta^3 D(\Omega_B/\delta)}{\Omega_B^3}, \quad (\text{D3})$$

$$\langle \sin^4(\theta_A) \rangle = \frac{3\delta^4 \Omega_B - (3\delta^5 + 2\Omega_B^2 \delta^3) D(\Omega_B/\delta)}{\Omega_B^5}. \quad (\text{D4})$$

It allows us to obtain an analytic expression for  $\langle \delta \mathcal{J}_0^2 \rangle$ :

$$\langle \delta \mathcal{J}_0^2 \rangle = J_1^2 \frac{\delta^3}{4\Omega_B^{12}} \left[ 2\delta \Omega_B^2 - (\delta^2 \Omega_B + 2\Omega_B^3) D\left(\frac{\Omega_B}{\delta}\right) - D^2\left(\frac{\Omega_B}{\delta}\right) \right] \left[ 36\delta^4 \Omega_B^2 - 24\delta^2 \Omega_B^4 + 8\Omega_B^6 - (45\delta^5 \Omega_B - 6\delta^3 \Omega_B^3) D\left(\frac{\Omega_B}{\delta}\right) + 9\delta^6 D^2\left(\frac{\Omega_B}{\delta}\right) \right]. \quad (\text{D5})$$

- [1] S. Forrest, The path to ubiquitous and low-cost organic electronic appliances on plastic, *Nature* **428**, 911 (2004).
- [2] Q. Wei, N. Fei, A. Islam, T. Lei, L. Hong, R. Peng, X. Fan, L. Chen, P. Gao, and Z. Ge, Small-molecule emitters with high quantum efficiency: Mechanisms, structures, and applications in OLED devices, *Adv. Opt. Mater.* **6**, 1800512 (2018).
- [3] C. J. Brabec, N. S. Sariciftci, and J. C. Hummelen, Plastic solar cells, *Adv. Funct. Mater.* **11**, 15 (2001).
- [4] R. Zhou, Z. Jiang, C. Yang, J. Yu, J. Feng, M. A. Adil, D. Deng, W. Zou, J. Zhang, K. Lu, W. Ma, F. Gao, and Z. Wei, All-small-molecule organic solar cells with over 14 efficiency by optimizing hierarchical morphologies, *Nat. Commun.* **10**, 5393 (2019).
- [5] B. Qiu, Z. Chen, S. Qin, J. Yao, W. Huang, L. Meng, H. Zhu, Y. (M.) Yang, Z.-G. Zhang, and Y. Li, Highly efficient all-small-molecule organic solar cells with appropriate active layer morphology by side chain engineering of donor

molecules and thermal annealing, *Adv. Mater.* **32**, 1908373 (2020).

- [6] H. Bässler and A. Köhler, Charge transport in organic semiconductors, in *Unimolecular and Supramolecular Electronics I: Chemistry and Physics Meet at Metal-Molecule Interfaces*, edited by R. M. Metzger (Springer, Berlin, Heidelberg, 2012), pp. 1–65.
- [7] I. I. Fishchuk, A. Kadashchuk, S. T. Hoffmann, S. Athanasopoulos, J. Genoe, H. Bässler, and A. Köhler, Unified description for hopping transport in organic semiconductors including both energetic disorder and polaron contributions, *Phys. Rev. B* **88**, 125202 (2013).
- [8] A. L. Efros and B. I. Shklovskii, *Electronic Properties of Doped Semiconductors* (Springer Science & Business Media, Berlin, 2013).
- [9] J. Kalinowski, M. Cocchi, D. Virgili, P. Di Marco, and V. Fattori, Magnetic field effects on emission and current in Alq3-

- based electroluminescent diodes, *Chem. Phys. Lett.* **380**, 710 (2003).
- [10] Ö. Mermer, G. Veeraraghavan, T. L. Francis, Y. Sheng, D. T. Nguyen, M. Wohlgenannt, A. Köhler, M. K. Al-Suti, and M. S. Khan, Large magnetoresistance in nonmagnetic  $\pi$ -conjugated semiconductor thin film devices, *Phys. Rev. B* **72**, 205202 (2005).
- [11] V. N. Prigodin, J. D. Bergeson, D. M. Lincoln, and A. J. Epstein, Anomalous room temperature magnetoresistance in organic semiconductors, *Synth. Met.* **156**, 757 (2006).
- [12] P. A. Bobbert, T. D. Nguyen, F. W. A. van Oost, B. Koopmans, and M. Wohlgenannt, Bipolaron Mechanism for Organic Magnetoresistance, *Phys. Rev. Lett.* **99**, 216801 (2007).
- [13] T. D. Nguyen, G. Hukic-Markosian, F. Wang, L. Wojcik, X.-G. Li, E. Ehrenfreund, and Z. V. Vardeny, Isotope effect in spin response of  $\pi$ -conjugated polymer films and devices, *Nat. Mater.* **9**, 345 (2010).
- [14] K. Schulten and P. G. Wolynes, Semiclassical description of electron spin motion in radicals including the effect of electron hopping, *J. Chem. Phys.* **68**, 3292 (1978).
- [15] I. A. Merkulov, A. L. Efros, and M. Rosen, Electron spin relaxation by nuclei in semiconductor quantum dots, *Phys. Rev. B* **65**, 205309 (2002).
- [16] D. S. Smirnov, E. A. Zhukov, D. R. Yakovlev, E. Kirstein, M. Bayer, and A. Greilich, Spin polarization recovery and Hanle effect for charge carriers interacting with nuclear spins in semiconductors, *Phys. Rev. B* **102**, 235413 (2020).
- [17] A. V. Shumilin, V. V. Kabanov, and V. I. Dediu, Magnetoresistance in organic semiconductors: Including pair correlations in the kinetic equations for hopping transport, *Phys. Rev. B* **97**, 094201 (2018).
- [18] A. V. Shumilin, Microscopic theory of organic magnetoresistance based on kinetic equations for quantum spin correlations, *Phys. Rev. B* **101**, 134201 (2020).
- [19] K. V. Kavokin, Spin relaxation of localized electrons in  $n$ -type semiconductors, *Semicond. Sci. Technol.* **23**, 114009 (2008).
- [20] D. S. Smirnov and L. E. Golub, Electrical Spin Orientation, Spin-Galvanic, and Spin-Hall Effects in Disordered Two-Dimensional Systems, *Phys. Rev. Lett.* **118**, 116801 (2017).
- [21] A. V. Shumilin, D. S. Smirnov, and L. E. Golub, Spin-related phenomena in the two-dimensional hopping regime in magnetic field, *Phys. Rev. B* **98**, 155304 (2018).
- [22] Y. Sheng, T. D. Nguyen, G. Veeraraghavan, Ö. Mermer, and M. Wohlgenannt, Effect of spin-orbit coupling on magnetoresistance in organic semiconductors, *Phys. Rev. B* **75**, 035202 (2007).
- [23] J.-Q. Zhao, M. Ding, T.-Y. Zhang, N.-Y. Zhang, Y.-T. Pang, Y.-J. Ji, Y. Chen, F.-X. Wang, and G. Fu, The effect of spin-orbit coupling on magnetoresistance in nonmagnetic organic semiconductors, *Chin. Phys. B* **21**, 057110 (2012).
- [24] A. S. Alexandrov, V. A. Dediu, and V. V. Kabanov, Hopping Magnetotransport via Nonzero Orbital Momentum States and Organic Magnetoresistance, *Phys. Rev. Lett.* **108**, 186601 (2012).
- [25] N. J. Harmon and M. E. Flatté, Semiclassical theory of magnetoresistance in positionally disordered organic semiconductors, *Phys. Rev. B* **85**, 075204 (2012).
- [26] N. J. Harmon and M. E. Flatté, Effects of spin-spin interactions on magnetoresistance in disordered organic semiconductors, *Phys. Rev. B* **85**, 245213 (2012).
- [27] A. Larabi and D. Bourbie, Correlated disordered electrons and organic magnetoconductance, *J. Appl. Phys.* **121**, 085502 (2017).
- [28] A. V. Shumilin and V. V. Kabanov, Kinetic equations for hopping transport and spin relaxation in a random magnetic field, *Phys. Rev. B* **92**, 014206 (2015).
- [29] A. Massé, P. Friederich, F. Symalla, F. Liu, V. Meded, R. Coehoorn, W. Wenzel, and P. A. Bobbert, Effects of energy correlations and superexchange on charge transport and exciton formation in amorphous molecular semiconductors: An *ab initio* study, *Phys. Rev. B* **95**, 115204 (2017).
- [30] R. Hanson, L. P. Kouwenhoven, J. R. Petta, S. Tarucha, and L. M. K. Vandersypen, Spins in few-electron quantum dots, *Rev. Mod. Phys.* **79**, 1217 (2007).
- [31] V. N. Mantsevich and D. S. Smirnov, Universal power law decay of spin polarization in double quantum dot, *Phys. Rev. B* **100**, 075409 (2019).
- [32] P. A. Bobbert, W. Wagemans, F. W. A. van Oost, B. Koopmans, and M. Wohlgenannt, Theory for Spin Diffusion in Disordered Organic Semiconductors, *Phys. Rev. Lett.* **102**, 156604 (2009).
- [33] D. R. McCamey, K. J. van Schooten, W. J. Baker, S.-Y. Lee, S.-Y. Paik, J. M. Lupton, and C. Boehme, Hyperfine-Field-Mediated Spin Beating in Electrostatically Bound Charge Carrier Pairs, *Phys. Rev. Lett.* **104**, 017601 (2010).
- [34] P. A. Bobbert, What makes the spin relax? *Nat. Mater.* **9**, 288–290 (2010).
- [35] Z. G. Yu, F. Ding, and H. Wang, Hyperfine interaction and its effects on spin dynamics in organic solids, *Phys. Rev. B* **87**, 205446 (2013).
- [36] M. M. Glazov, *Electron and Nuclear Spin Dynamics in Semiconductor Nanostructures* (Oxford University Press, Oxford, England, 2018).
- [37] A. V. Shumilin and D. S. Smirnov, Nuclear Spin Dynamics, Noise, Squeezing, and Entanglement in Box Model, *Phys. Rev. Lett.* **126**, 216804 (2021).
- [38] M. A. Baldo and S. R. Forrest, Interface-limited injection in amorphous organic semiconductors, *Phys. Rev. B* **64**, 085201 (2001).
- [39] S. P. Kersten, A. J. Schellekens, B. Koopmans, and P. A. Bobbert, Magnetic-Field Dependence of the Electroluminescence of Organic Light-Emitting Diodes: A Competition between Exciton Formation and Spin Mixing, *Phys. Rev. Lett.* **106**, 197402 (2011).
- [40] E. Ehrenfreund and Z. V. Vardeny, Effects of magnetic field on conductance and electroluminescence in organic devices, *Isr. J. Chem.* **52**, 552 (2012).
- [41] S. A. Crooker, F. Liu, M. R. Kelley, N. J. D. Martinez, W. Nie, A. Mohite, I. H. Nayyar, S. Tretiak, D. L. Smith, and P. P. Ruden, Spectrally resolved hyperfine interactions between polaron and nuclear spins in organic light emitting diodes: Magneto-electroluminescence studies, *Appl. Phys. Lett.* **105**, 153304 (2014).
- [42] F. Liu, M. R. Kelley, S. A. Crooker, W. Nie, A. D. Mohite, P. P. Ruden, and D. L. Smith, Magneto-electroluminescence of organic heterostructures: Analytical theory and spectrally resolved measurements, *Phys. Rev. B* **90**, 235314 (2014).
- [43] J. Kurkijärvi, Conductivity in random systems. II. Finite-size-system percolation, *Phys. Rev. B* **9**, 770 (1974).

- [44] B. I. Shklovskii and A. L. Efros, The preexponential factor of hopping conduction, *Sov. Phys. JETP Lett.* **1**, 83 (1975).
- [45] J. Cottaar, L. J. A. Koster, R. Coehoorn, and P. A. Bobbert, Scaling Theory for Percolative Charge Transport in Disordered Molecular Semiconductors, *Phys. Rev. Lett.* **107**, 136601 (2011).
- [46] N. Fröhling, F. B. Anders, and M. Glazov, Nuclear spin noise in the central spin model, *Phys. Rev. B* **97**, 195311 (2018).
- [47] Ph. Glasenapp, D. S. Smirnov, A. Greulich, J. Hackmann, M. M. Glazov, F. B. Anders, and M. Bayer, Spin noise of electrons and holes in (In,Ga)As quantum dots: Experiment and theory, *Phys. Rev. B* **93**, 205429 (2016).
- [48] A. V. Shumilin, E. Ya. Sherman, and M. M. Glazov, Spin dynamics of hopping electrons in quantum wires: Algebraic decay and noise, *Phys. Rev. B* **94**, 125305 (2016).
- [49] D. S. Smirnov, V. N. Mantsevich, and M. M. Glazov, Theory of optically detected spin noise in nanosystems, [arXiv:2010.15763](https://arxiv.org/abs/2010.15763) [*Phys. Usp.* (to be published)].